Physics and Astronomy Reports
PAR 2024, 2 (1), 18–28
DOI: 10.26650/PAR.2024.00003

RESEARCH ARTICLE

The Fundamental Parameters and Evolutionary Status of V454 Aurigae

G. Yücel[1*], R. Canbay[2], and V. Bakış[3]

[1]İstanbul University, Faculty of Science, Department of Astronomy and Space Sciences, Beyazıt, 34119, İstanbul, Türkiye
[2]İstanbul University, Institute of Graduate Studies in Science, Programme of Astronomy and Space Sciences, 34116, Beyazıt, İstanbul, Türkiye
[3]Akdeniz University, Faculty of Science, Department of Space Sciences and Technologies, Konyaaltı, 07030, Antalya, Türkiye

ABSTRACT

Eclipsing binary systems have a unique feature that enables scientists to obtain precise fundamental star parameters, which opens up a greater area of astrophysics studies. In this study, we derived the fundamental parameters, evolutionary status, and birthplace of V454 Aur in the Galaxy by combining radial velocity, photometric, and spectral energy distribution data. We have updated the ephemerides and period of V454 Aur as $2458850.80136^{+0.00001}_{-0.00001}$ and $27.0198177^{+0.0000003}_{-0.0000003}$, respectively. We obtain $1.173^{+0.016}_{-0.016}$ $M_\odot$ and $1.203^{+0.022}_{-0.026}$ $R_\odot$ for the primary component and $1.045^{+0.015}_{-0.014}$ $M_\odot$ and $0.993^{+0.034}_{-0.027}$ $R_\odot$ for the secondary component. The effective temperatures for the components were accurately determined via SED data as 6250^{+150}_{-150} K and 5966^{+109}_{-89} K for the primary component and secondary component, respectively. The metallicity of the components is derived from evolutionary tracks, which implies a slightly higher metallicity than Solar metallicity. According to the analysis, the components of V454 Aur are in the main sequence. Our distance calculation for the system is 65.07^{+2}_{-3} pc and is in excellent agreement with *Gaia* astrometric data, which is $65.07^{+0.09}_{-0.09}$ pc. The current age of the system is $1.19^{+0.08}_{-0.09}$ Gyr, and it will start mass transfer between components in 5 Gyr from now on. Dynamical orbital analysis shows that V454 Aur follows a boxy pattern around the Galactic centre and is a member of the thin-disc component of the Galaxy. Considering the age and metallicity of this system, it was found to have formed just outside the Solar circle.

Keywords: Stars: binaries ; stars: fundamental parameters ; stars: evolution ; stars: kinematics

1. INTRODUCTION

In principle, to understand our Galaxy, and therefore the universe, and its evolution, we need to understand its cornerstone, which is stars. The evolution of a star is mostly based on its mass, and then its chemical composition. There are several ways to acquire the mass of a star, but among them, eclipsing binaries are the most accurate ones (Serenelli et al. 2021). Eclipsing binaries, in general, are the centre of astrophysics studies because they provide valuable information (mass, radius, temperature, etc.) of the component stars within 1-3% uncertainty rates, or mostly even better according to the quality of the data used in analysis (Torres et al. 2010; Prša 2020). The number of eclipsing binaries with known fundamental parameters is increasing every day, but this is not a reason to stop investigating new eclipsing binary systems and obtaining their parameters, since every known system is a source for several studies from stellar populations (e.g. Chabrier 2003; Moe & Di Stefano 2017) to empirical MLR studies (e.g. Benedict et al. 2016; Eker et al. 2015, 2018, 2024). Therefore, there is still a need to study eclipsing binaries and derive their fundamental parameters precisely.

V454 Aur (HD 44192, SAO 59016, Hip 30270, l = 178°.803546, b = 09°.510553) is a Northern Hemisphere detached eclipsing binary system. The variable star feature of V454 Aur was discovered by *Hipparcos* (Perryman et al. 1997). The first ground-based observation of V454 Aur was done by Griffin (2001) via obtaining photoelectric radial velocities (RVs). As a result, the spectroscopic orbit of V454 Aur was calculated. Later, Nordström et al. (2004) calculated the temperature, metallicity, and age of the star as 6025 K, -0.14 dex, and 5 Gyr, respectively, by using *ubvy* photometric data. These values were improved by Holmberg et al. (2009) and later on by Casagrande et al. (2011) for temperature, log g, metallicity, and age as 6064 K, -0.08 dex, 4.43 dex, and 4 Gyr, respectively. Prša et al. (2022) have used *TESS* (Ricker et al. 2015) observations to calculate ephemerides and the period of V454 Aur and obtained the values of 2458850.778358±0.002306 and 17.8883306±0.0064858 days, respectively. However, they performed the analysis based on only one sector, the 20th. There has been no prior study of this system.

In this study, we combined radial velocity and photometric data with multiple sectors, which is provided by *TESS*, and obtained the fundamental parameters of V454 Aur for the first

Corresponding Author: G. Yücel **E-mail:** gokhannyucel@gmail.com

Submitted: 07.03.2024 • **Revision Requested:** 12.04.2024 • **Last Revision Received:** 26.04.2024 • **Accepted:** 28.04.2024 • **Published Online:** 05.06.2024

time in the literature. We studied its evolution scenarios and found the system's initial orbital parameters and kinematics, which tell us where this system was born.

This paper is structured as follows. In Section 2, we present the properties of the observational data used. In Section 3, the calculated fundamental parameters of the system are presented. In Section 4, we present a detailed evolutionary analysis. In Section 5, we present the kinematics of the system. Finally, in Section 6, we have discussed our comprehensive results.

2. DATA

2.1. Radial Velocities

Radial velocity data (RVs) used in this study, were taken from Griffin (2001). Details can be found in that paper, but we briefly give a summary here. Griffin (2001) observed V454 Aur in the years of 2000-2001, with a total of 65 observations for both components at Observatoire de Haute-Provence[1] with 1-m Swiss telescope, equipped with Coravel (Baranne et al. 1979) instrument. The RVs used in this study are given in Table 1.

2.2. Photometric Data

Photometric data, which are used in this study, have been obtained via *TESS*. Although the main purpose of *TESS* is that of finding exoplanets by looking at brightness changes of a star, it has also been a source of producing light curves of eclipsing binaries, which are also needed to analyse eclipsing binary systems (Prša et al. 2022).

TESS has observed V454 Aur in a total of five sectors, which are 20, 43, 44, 45, and 60 with exposure times 1800s, 600s, 600s, 600s, and 200s, respectively. *TESS* has also observed V454 Aur in sectors 71, 72, and 73, but those photometric data are not available.

We have used `Lightkurve` v2.4 (Lightkurve Collaboration et al. 2018) to acquire photometric data. Photometric data with 200s exposure time were used in the analysis wherever available, but missing parts were completed by other sectors. The photometric data used in this study are shown in Figure 1 by each sector.

3. FUNDAMENTAL PARAMETERS

3.1. Analysis of Ephemerides

In the literature, there is only one time of minimum measurement, which was obtained with *Hipparcos* (Perryman et al. 1997), for the system, which makes its long-term orbital period change study impossible. Nevertheless, *TESS* satellite obtained five consecutive measurements (sectors; see Figure 1),

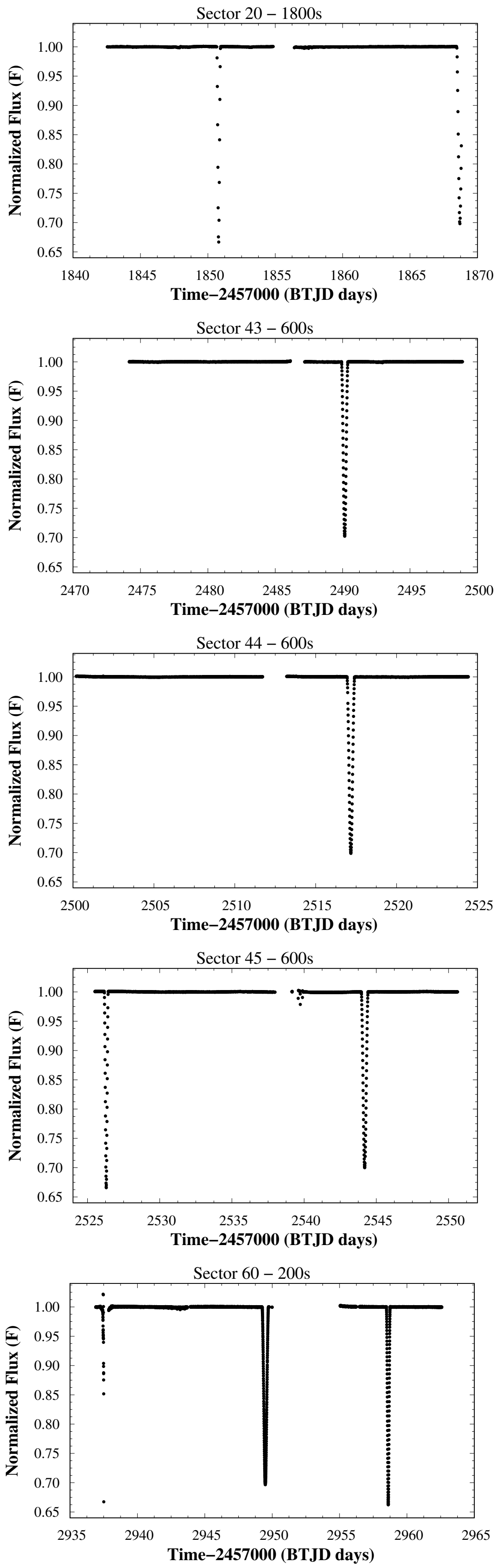

Figure 1. *TESS* observation of V454 Aur in five different sectors.

[1] http://www.obs-hp.fr

Table 1. The radial velocities that were used in this study.

HJD-2400000	RV_1 (km s^{-1})	RV_2 (km s^{-1})	HJD-2400000	RV_1 (km s^{-1})	RV_2 (km s^{-1})	HJD-2400000	RV_1 (km s^{-1})	RV_2 (km s^{-1})
51595.994	-29.3	-52.5	51852.055	-54.1	-24.5	51906.102	-54.1	-24.6
51602.935	-76.8	0.0	51852.097	-53.6	-27.0	51906.115	-54.6	-25.0
51604.912	-93.2	20.0	51852.149	-52.6	-26.3	51906.128	-54.3	-24.9
51606.817	-95.2	22.9	51852.199	-51.5	-29.5	51906.141	-54.8	-24.0
51607.009	-92.9	–	51852.253	-50.8	-31.2	51908.029	-21.2	-64.3
51607.936	-76.0	0.6	51861.198	-11.1	-73.4	51908.894	-13.2	-72.4
51609.912	-33.1	-48.2	51863.154	-16.7	-66.5	51916.051	-13.0	-71.2
51624.908	-38.9	-42.0	51865.156	-25.4	-58.7	51917.973	-19.3	-64.2
51627.947	-60.2	-18.1	51870.143	–	-27.3	51918.947	-24.4	-59.6
51628.889	-67.8	-9.8	51870.225	–	-25.5	51920.099	-29.4	-54.0
51639.886	-7.0	-77.0	51870.268	-54.0	-25.7	51922.976	-44.6	-36.0
51640.896	-5.2	-79.8	51878.126	-77.0	0.6	51924.956	-58.6	-19.9
51641.857	-5.4	-79.4	51880.176	-31.7	-47.5	51925.961	-67.1	-10.8
51657.870	-85.8	10.3	51881.096	-19.1	-62.7	51926.926	-74.4	-4.0
51660.892	-95.1	21.0	51887.089	-7.6	-76.2	51934.972	-21.8	-62.7
51812.171	-29.4	-51.4	51892.066	-23.7	-58.7	51936.957	-7.8	-77.3
51823.191	-93.3	18.8	51900.062	-76.2	-0.8	51946.977	-27.9	-53.8
51826.158	-32.3	-50.8	51906.057	-55.6	-23.8	51954.959	-84.2	8.5
51834.181	-10.9	-72.6	51906.068	-55.4	-24.0	51956.851	-97.7	24.7
51851.043	-78.2	1.7	51906.080	-55.0	-23.8	51981.946	-83.7	8.5
51851.972	-57.0	-22.0	51906.091	-55.3	-24.6			

and using *TESS* measurements allows us to determine the up-to-date ephemeris of the system. We measured the times of minima available in the *TESS* photometric data using the Kwee-Van Woerden method (Kwee & van Woerden 1956), which are presented in Table 2. Because the system has an eccentric orbit, primary and secondary ephemerides are calculated separately. The linear least-squares method to the $O-C$ data ($O-C = T-(T_0+P\times E)$) yielded the following ephemerides:

$$T(\text{HJD}) = 2458850.80136(1) + 27.0198177(3)\times E \quad (1)$$

for the primary minimum,

$$T(\text{HJD}) = 2458868.69867(61) + 27.0198105(233)\times E \quad (2)$$

for the secondary minimum. The $O-C$ diagram is shown in Figure 2.

Table 2. The times of minima of V454 Aur extracted from *TESS* data.

Times of minima (HJD)	Component
2458850.80135	pri
2458868.69850	sec
2459490.15397	sec
2459517.17517	sec
2459526.29680	pri
2459544.19366	sec
2459949.49083	sec
2459958.61390	pri
2460255.83187	pri
2460282.85168	pri

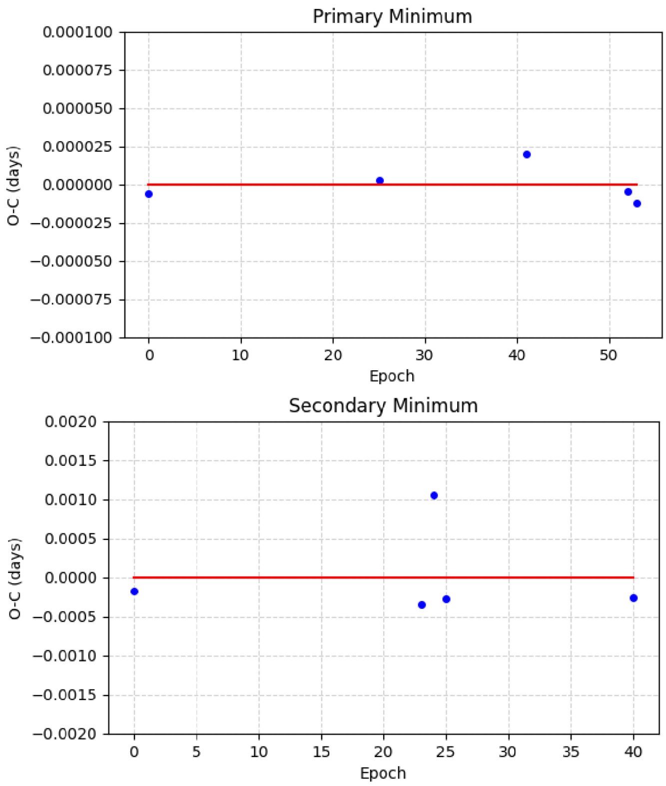

Figure 2. $O-C$ diagram for primary and secondary minima.

3.2. Spectroscopic Orbit and Light Curve Modelling

Although the spectroscopic orbit of V454 Aur has been calculated by Griffin (2001), the system has been reanalysed with simultaneous solutions using both RV data and photometric data to obtain fundamental parameters such as mass, radius, temperature ratio, and the light contributions of both components using PHysics Of Eclipsing BinariEs v1.0[2] (PHOEBE, Prša & Zwitter 2005) which is based on Wilson-Devinney code (WD, Wilson & Devinney 1971; Wilson 1979, 1990; van Hamme 1993; van Hamme & Wilson 2003).

Since there is no indication in the photometric data of any mass transfer in the system, the analysis was performed in detached mode. During the analysis, conjunction time T_0, orbital period P, and the temperature of the primary component were fixed (see the next section for how the primary component's temperature has been determined) and the following parameters were adjusted: mass ratio (q), eccentricity (e), the argument of periapsis (w), semi-major axis (a), systemic velocity (V_γ), orbital inclination (i), temperature of secondary component (T_2), dimensionless surface potentials of both components ($\Omega_{1,2}$), and monochromatic luminosity (L_1). For the limb-darkening (LD) calculations, we adopted logarithmic LD laws. LD values were calculated from Fortran code written by Walter van Hamme[3].

After the initial analysis, we used a custom Markov chain Monte Carlo (MCMC) sampler[4] based on `emcee` (Foreman-Mackey et al. 2013) to improve the parameters of the components of V454 Aur and to determine the heuristic errors. The sampler ran with 128 walkers and 1000 iterations as conventional. The LC and spectroscopic orbit models are presented in Figure 3 and the fundamental parameters and heuristic errors for V454 Aur are presented in Table 3.

3.3. Component Temperatures

The *Gaia* DR3 trigonometric parallax of V454 Aur is ϖ = 15.3669 ± 0.0217 mas, corresponding to a distance of 65.07 ± 0.09 pc. At this distance, it is expected to be a negligible interstellar extinction. Therefore, the observed $B-V$ colour indicates an extinction-free colour and helps in preliminary temperature estimation. The observed $B-V$ of V454 Aur is given to be 0.57 mag corresponding to a temperature of 5879 K using the colour-$T_{\rm eff}$ calibration table in Bakış & Eker (2022). It should be noted that this colour is the combined colour of two components, making the primary component seem cooler. To obtain a more reliable temperature estimation of the components, we obtained the SED data of V454 Aur and modelled it with the Planck curve as described in Bakış & Eker (2022). While modelling the SED data, the temperature ratio obtained from the LC analysis, the absolute radii of the components, and the distance to V454 Aur are fixed. In Figure 4, we show the SED data of V454 Aur and the best-fitting Planck curve. The temperatures of the components are determined to be 6250 K and 5966 K for the primary and secondary components, respectively. The corner plot of the posterior distribution of the fundamental parameters of V454 Aur is presented in Figure 5.

[2] http://phoebe-project.org/1.0/download
[3] https://faculty.fiu.edu/~vanhamme/ldfiles/ldinterpol.for
[4] https://sourceforge.net/p/phoebe/mailman/message/33650955/

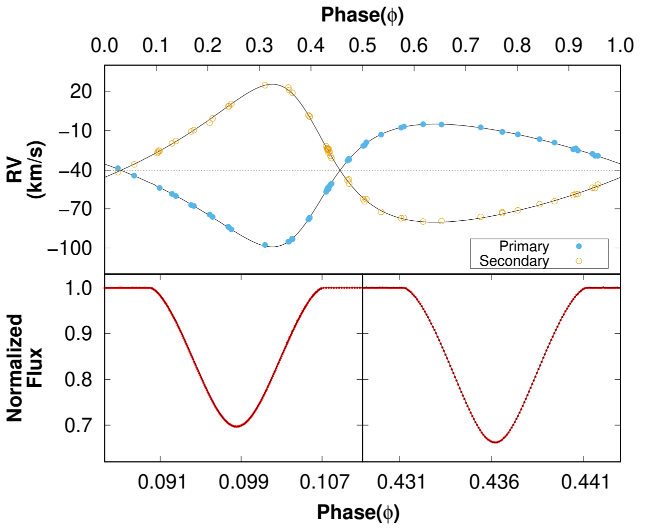

Figure 3. Observed RVs with best fitting radial velocity curves and photometric data with LC modelling. Blue and yellow circles represent the RVs of the primary and secondary components of V454 Aur, respectively. In LC modelling, red dots represent the photometric data and the black curve is the best LC model.

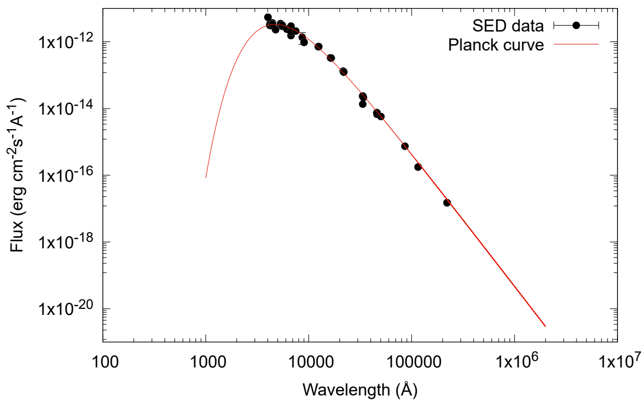

Figure 4. SED data and the Planck curve with binary parameters. The figure axes are in log scale. The SED data corresponds to within 1 arcsec around V454 Aur.

4. EVOLUTIONARY ANALYSIS

One of the scopes of this study is to determine the evolution scenario for V454 Aur using the fundamental parameters we obtained. In this regard, we have used the version of r23.05.1 of Modules for Experiments in Stellar Astrophysics (MESA Paxton et al. 2011, 2013, 2015, 2018, 2019; Jermyn et al. 2023) and MESA SDK v23.7.3 (Townsend 2024) to calculate the evolution of V454 Aur. `MESA` uses a bunch of microphysics data created by several researchers. The MESA EOS is a blend of the OPAL (Rogers & Nayfonov 2002), SCVH (Saumon et al. 1995), FreeEOS (Irwin 2004), HELM (Timmes & Swesty 2000), PC (Potekhin & Chabrier 2010), and Skye (Jermyn et al. 2021) EOSes. Radiative opacities are primarily from OPAL (Iglesias & Rogers 1993, 1996), with low-temperature data from Ferguson et al. (2005) and the high-temperature, Compton-scattering dominated regime by Poutanen (2017). Electron conduction opacities are from Cassisi et al. (2007) and Blouin et al. (2020).

Table 3. Binary stellar parameters and heuristic errors of V454 Aur.

Parameter	Symbol	Primary	Secondary
Spectral type	Sp	F1 V-IV	F1 V-IV
Ephemerides time (d)	T_0	$2458850.80136^{+0.00001}_{-0.00001}$	
Orbital period (d)	P	$27.0198177^{+0.0000003}_{-0.0000003}$	
Mass ($M_\odot$)	M	$1.173^{+0.016}_{-0.016}$	$1.045^{+0.015}_{-0.014}$
Radius ($R_\odot$)	R	$1.203^{+0.022}_{-0.026}$	$0.993^{+0.034}_{-0.027}$
Surface gravity (cgs)	$\log g$	$4.345^{+0.025}_{-0.022}$	$4.465^{+0.031}_{-0.035}$
Separation ($R_\odot$)	a	$49.418^{+0.173}_{-0.167}$	
Orbital inclination (°)	i	$89.263^{+0.025}_{-0.027}$	
Mass ratio	q	$0.890^{+0.006}_{-0.005}$	
Eccentricity	e	$0.37717^{+0.00016}_{-0.00013}$	
Argument of perigee (rad)	w	$3.99763^{+0.00035}_{-0.00035}$	
Light Ratio (*TESS*)	$l/l_{\rm total}$	$0.631^{+0.013}_{-0.018}$	$0.369^{+0.018}_{-0.013}$
Temperature (K)	$T_{\rm eff}$	$6250^{+0.150}_{-0.150}$	$5966^{+0.109}_{-0.089}$
Luminosity ($L_\odot$)	$\log L$	$0.297^{+0.057}_{-0.061}$	$0.050^{+0.055}_{-0.056}$
Metallicity	z	$0.017^{+0.002}_{-0.002}$	
Combined visual magnitude[1]	*TESS*	$7.131^{+0.006}_{-0.006}$	
Individual visual magnitude	$TESS_{1,2}$	$7.631^{+0.022}_{-0.022}$	$8.213^{+0.038}_{-0.038}$
Combined visual magnitude	V	$7.65^{+0.01}_{-0.01}$	
Individual visual magnitude	$V_{1,2}$	$8.129^{+0.025}_{-0.025}$	$8.768^{+0.040}_{-0.040}$
Combined colour index (mag)	$B-V$	$0.57^{+0.03}_{-0.03}$	
Colour excess (mag)	$E(B-V)$	0	
Bolometric magnitude	$M_{\rm bol}$	$4.010^{+0.163}_{-0.167}$	$4.625^{+0.220}_{-0.223}$
Absolute visual magnitude	$M_{\rm V}$	$4.025^{+0.153}_{-0.157}$	$4.676^{+0.211}_{-0.215}$
Bolometric correction (mag)[2]	$BC_{\rm TESS}$	$0.440^{+0.006}_{-0.005}$	$0.490^{+0.009}_{-0.007}$
Bolometric correction (mag)[3]	$BC_{\rm V}$	$0.093^{+0.009}_{-0.008}$	$0.083^{+0.011}_{-0.006}$
Systemic velocity (km s^{-1})	v_γ	$-40.480^{+0.099}_{-0.104}$	
Computed synchronisation velocity (km s^{-1})	$v_{\rm synch}$	$2.1^{+0.1}_{-0.1}$	$1.9^{+0.1}_{-0.1}$
Age (Gyr)	t	$1.19^{+0.08}_{-0.09}$	
Distance (pc)	d	65^{+2}_{-3}	
Gaia distance (pc)	d	65.07 ± 0.09	

[1]Paegert et al. (2022),[2]Eker & Bakış (2023),[3]Bakış & Eker (2022)

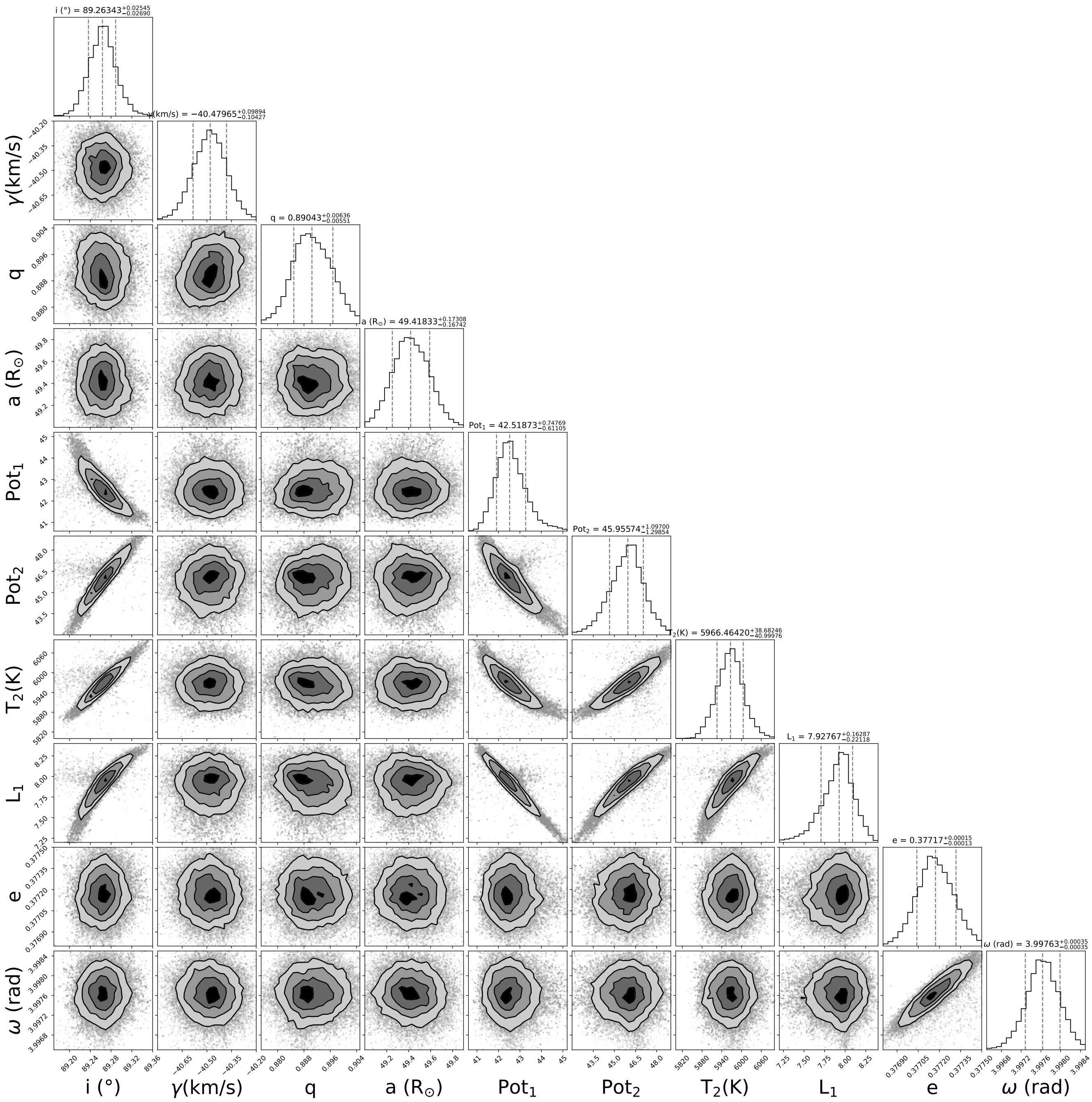

Figure 5. A corner plot of the posteriors for the fundamental parameters of V454 Aur.

Nuclear reaction rates are from JINA REACLIB (Cyburt et al. 2010), NACRE (Angulo et al. 1999) and additional tabulated weak reaction rates Fuller et al. (1985); Oda et al. (1994); Langanke & Martínez-Pinedo (2000). Screening is included via the prescription of Chugunov et al. (2007). Thermal neutrino loss rates are from Itoh et al. (1996), Roche lobe radii in binary systems are computed using the fit of Eggleton (1983). Mass transfer rates in Roche lobe overflowing binary systems are determined following the prescription of Ritter (1988), and so on.

The evolutionary scenario of V454 Aur was studied in two sections: single-star evolution and binary-star evolution.

4.1. Single-star evolution

To establish a well-calculated evolution scenario for a star or a system, the metallicity of the star/system must be known and calculations should be performed according to it. Because there is no spectroscopic data for V454 Aur, we have chosen evolution tracks to determine the metallicity of the systems. Eclipsing binary systems were born in the same stellar nurseries/associations, hence, the metallicity of the components of a binary system must be the same/identical. Considering that the system is detached and there is no mass transfer between components, the components can be treated as individual stars. By using `MESA`, by including the calculated mass of the components of V454 Aur, we built a grid of evolutionary tracks with different metallicities and, ZAMS lines, which are dashed lines. Our results are given in Figure 6 as $T_{\rm eff} - \log L$, $T_{\rm eff} - R$, and $T_{\rm eff} - \log g$ planes. Hence, the metallicity (z) of the system was determined as $z = 0.017 \pm 0.002$. Both components of V454 Aur are in the main sequence and still burning hydrogen in their cores.

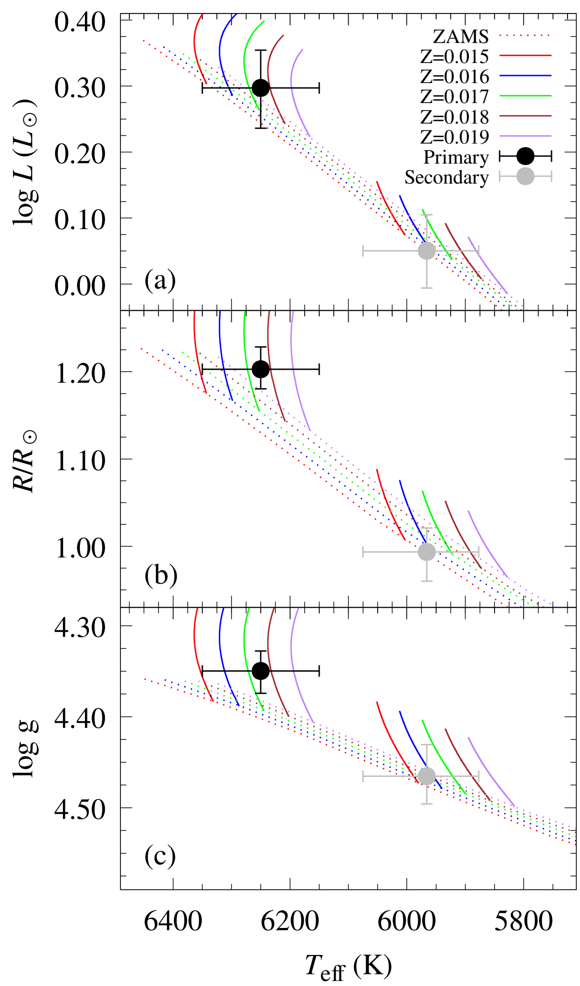

Figure 6. Single star evolutionary tracks with different metallicities for V454 Aur on (a) $T_{\rm eff}$–$\log L$ plane, (b) $T_{\rm eff}$–R plane, and (c) $T_{\rm eff}$–$\log g$ plane, respectively.

4.2. Binary-star evolution

The components of V454 Aur are on the main-sequence and the system is detached. Hence, the calculation of the evolution of the system with single-star evolution is agreeable. Nonetheless, to understand the evolution of the system from its formation to its end, it is necessary to evolve the system in binary form. `MESA` enables this option with its `binary` module. As a starting point, the initial orbital conditions must be calculated. In this regard, we have used a similar approach that has already been used in literature (Rosales et al. 2019; Soydugan et al. 2020; Yücel & Bakış 2022). We built a grid with starting different initial orbital periods and different initial orbital eccentricities and ran the evolution with each model until the orbital eccentricity dropped to the current eccentricity value of V454 Aur. Then, a χ^2 calculation was performed using the determined orbital period of the system, calculated radii, and temperature of the components with every model in the grid. In our calculations, we have activated the option of magnetic breaking (Rappaport et al. 1983), since the components of V454 Aur have convective atmospheres. For the tidal synchronisation, we used the "Orb_period" option, which synchronises the orbit relevant to the timescale of the orbital period. We also applied tidal circularisation, given by Hurley et al. (2002).

In the grid, the evolution models that the initial parameters change for the period and eccentricity between 27.020 and 27.040 d with an interval of 0.001 d and between 0.377190 and 0.377300 with an interval of 0.000005, respectively. We performed the evolution for each model and continued the evolution until eccentricity dropped to 0.377170, which is the up-to-date eccentricity value of V454 Aur. The best model gives, the lowest χ^2, 0.00016, with initial orbital parameters for period and eccentricity of 27.021 and 0.377210, respectively (given in Figure 7).

Later, we started binary evolution with the determined initial orbital parameters and evolved the system until the primary star started mass transfer. According to our calculations, the age of the V454 Aur is 1.19±0.09 Gyr. Taking the system as 6.23 Gyr, the mass transfer will start from the primary star, which will be on the red giant branch, to the secondary star, which will still

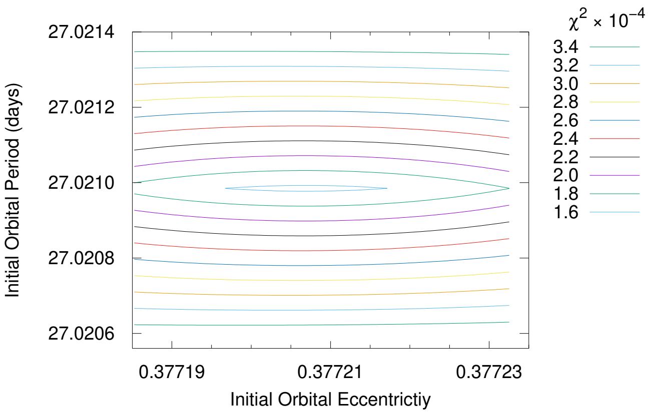

Figure 7. χ^2 map of the corresponding initial period for each initial orbital eccentricity of V454 Aur.

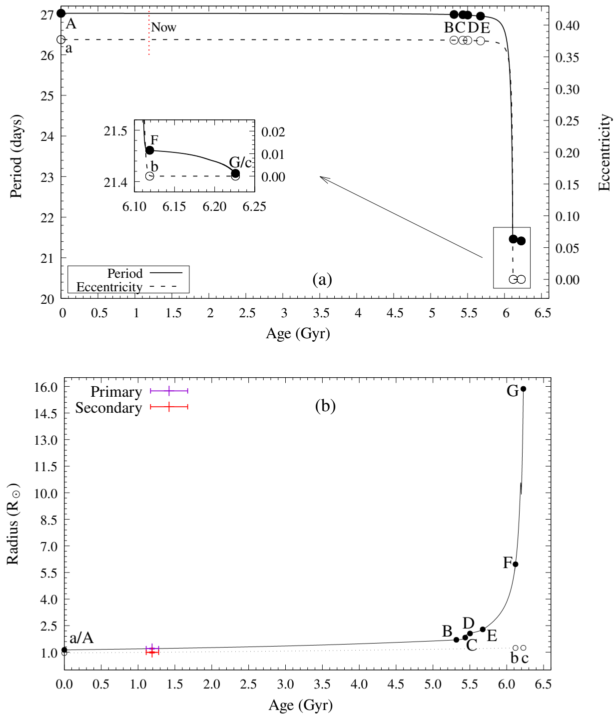

Figure 8. Change of orbital parameters (a), and radius of the components (b) of V454 Aur with time.

be on the main sequence. Changes in the orbital parameters and radii of the components during evolution are presented in Figure 8. Detailed evolution of both components of V454 Aur with timetables are given in Table 4 and shown in Figure 9.

5. KINEMATICS AND GALACTIC ORBIT PARAMETERS

At the beginning of the *Gaia* era, the sensitivity of astrometric measurements of stars in the Solar neighbourhood has increased. This enabled a more precise determination of the kinematic and dynamic orbital parameters of nearby stars. In this study, we have focussed on the analysis of V454 Aur, determining its space velocity components and Galactic orbital parameters. The proper motion components and trigonometric parallaxes of the system were obtained from the *Gaia* DR3 database (Gaia Collaboration et al. 2023), and the centre-of-mass velocities of the V454 Aur system, as determined in this study, are presented in Table 5.

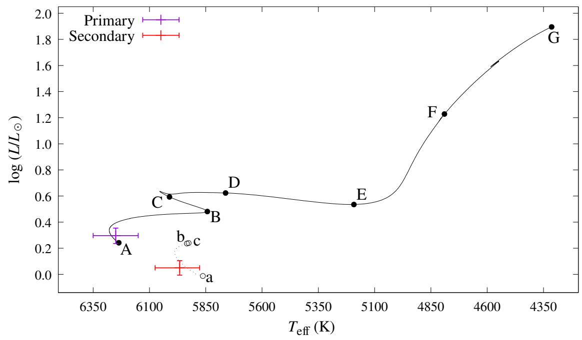

Figure 9. Evolution of V454 Aur on $T_{\rm eff}$ –log $L/L_\odot$ diagram.

The `galpy` code developed by Bovy (2015) was used to calculate the space velocity components for V454 Aur, and the uncertainties associated with these components were determined using the algorithm proposed by Johnson & Soderblom (1987). These space velocity components inherently incorporate biases due to the position of stars in the Milky Way and observations from the Sun. To correct for these biases, differential rotation and local standard rest (LSR) corrections have been applied to the velocity components of the stars. Differential rotational corrections for V454 Aur were applied using the equations mentioned by Mihalas & Binney (1981), obtaining velocity corrections of 0.04 and -0.15 km s^{-1} for the U and V space velocity components of the system, respectively. The W space velocity component, which is unaffected by differential rotation, was not corrected. For the LSR correction, the values of Coşkunoğlu et al. (2011) $(U,V,W)_\odot$ = $(8.83 \pm 0.24, 14.19 \pm 0.34, 6.57 \pm 0.21)$ km s^{-1} were considered, and the LSR values were extracted from the space velocity components for which a differential velocity correction was applied. The relation $S_{\rm LSR} = \sqrt{U^2_{\rm LSR} + V^2_{\rm LSR} + W^2_{\rm LSR}}$ was used to calculate the total space velocity ($S_{\rm LSR}$) of the system, and the results are listed in Table 5. Considering the total space velocity and space velocity components of the V454 Aur, it is consistent with the value given for the young thin-disc population (Leggett 1992).

The `galpy` code (Bovy 2015) was also used to compute the Galactic orbital parameters of the V454 Aur. For the Galactic potentials needed for the Galactic orbit calculations, `MWPotential2014` was used, which was created specifically for the Galaxy. For the system to form closed orbits around the Galactic centre, a timescale of 3 Gyr in 2 Myr steps was used. The Galactic orbital calculations resulted in the determination of several parameters, including the perigalactic distance ($R_{\rm p}$),

Table 4. Detailed evolution of V454 Aur with time-stamps.

Comp	Mark	Evolutionary Status	Age (Gyr)	P (day)	e	Primary			Secondary		
						$T_{\rm eff}$ (K)	$\log L$ ($L_\odot$)	R ($R_\odot$)	$T_{\rm eff}$ (K)	$\log L$ ($L_\odot$)	R ($R_\odot$)
Pri	A	ZAMS	0	27.021	0.37721	6236	0.242	1.131	5863	-0.013	0.955
	B	Core contraction	5.32	26.991	0.37628	5843	0.481	1.699	5973	0.208	1.187
	C	TAMS	5.44	26.986	0.37615	6011	0.593	1.825	5969	0.213	1.194
	D	Thin H shell burning	5.50	26.978	0.37593	5762	0.623	2.056	5967	0.215	1.199
	E	Entering red giant phase	5.68	26.951	0.37519	5192	0.535	2.289	5959	0.221	1.210
	F	Circularisation of orbit	6.12	21.461	0	4790	1.228	5.968	5934	0.236	1.241
	G	Starting of mass transfer	6.23	21.416	0	4314	1.895	15.866	5926	0.240	1.248
Sec	a	ZAMS	0	27.021	0.37721	6236	0.242	1.131	5863	-0.013	0.955
	b	Circularisation of orbit	6.12	21.461	0	4790	1.228	5.968	5934	0.236	1.241
	c	Starting of mass transfer	6.23	21.416	0	4314	1.895	15.866	5926	0.240	1.248

Table 5. Astrometric and radial velocity of V454 Aur and calculated space velocity components and Galactic orbital parameters of the system.

Input Parameters								
Star	α (J2000) (hh:mm:ss)	δ (J2000) (dd:mm:ss)	$\mu_\alpha \cos\delta$ (mas yr^{-1})	μ_δ (mas yr^{-1})	ϖ (mas)	Ref	V_γ (km s^{-1})	Ref
V454 Aur	06:22:03.06	34:35:50.46	-0.514±0.025	-66.008±0.019	15.367±0.022	[1]	-40.48±0.10	[2]

Output Parameters								
Star	$U_{\rm LSR}$ (km s^{-1})	$V_{\rm LSR}$ (km s^{-1})	$W_{\rm LSR}$ (km s^{-1})	$S_{\rm LSR}$ (km s^{-1})	$R_{\rm a}$ (pc)	$R_{\rm p}$ (pc)	$Z_{\rm max}$ (pc)	e
V454 Aur	46.80±0.10	-4.61±0.03	-9.22±0.02	47.92±0.11	10038±40	7044±20	370±1	0.175±0.001

Ref: [1] Gaia Collaboration et al. (2023), [2] This study

apogalactic distance ($R_{\rm a}$), maximum distance from the Galactic plane ($Z_{\rm max}$), and eccentricity (e) of the Galactic orbits. These parameters are also listed in Table 5. The positions of the system according to their distances from the Galactic centre ($R_{\rm gc}$) and perpendicular to the Galactic plane (Z) at different times are shown in Figure 10a. The `galpy` results show that the V454 Aur has a slightly flattened Galactic orbit. Moreover, the fact that the system is at $Z = 11$ pc ($Z = d \times \sin b$) from the Galactic plane indicates that V454 Aur may belong to the young thin-disc component of Milk Way (Tunçel Güçtekin et al. 2019).

Galactic orbits for the V454 Aur system on $Z \times R_{\rm gc}$ and $R_{\rm gc} \times t$ diagrams are shown in Figure 10. The panels in Figure 10 show side views of the V454 Aur motions as functions of distance from the Galactic centre and the Galactic plane, respectively (Tasdemir & Yontan 2023). In Figure 10b the birth and present-day positions of V454 Aur are shown with yellow-filled triangles and circles, respectively (Yontan et al. 2022). The eccentricity of the orbit of the V454 Aur does not exceed the value of 0.18. The distances from the Galactic plane reach a maximum at $Z_{\rm max} = 370 \pm 1$ pc for V454 Aur. These results show that the V454 Aur belongs to the young thin disc of the Milky Way. The birthplace of the system was also investigated by running the binary system age ($t = 1.19 \pm 0.08$ Gyr) calculated in this work back in time using the `galpy` programme (Yontan & Canbay 2023). The birth radius of the

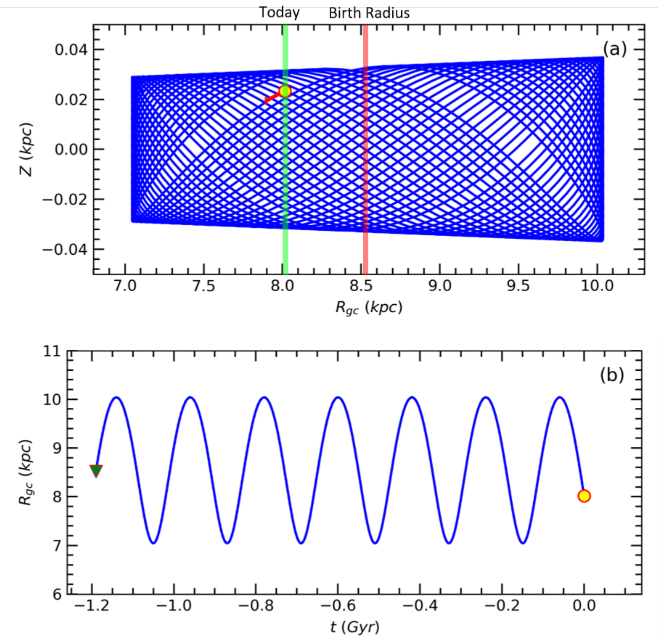

Figure 10. The Galactic orbits and birth radii of V454 Aur in the $Z \times R_{\rm gc}$ (a) and $R_{\rm gc} \times t$ (b) diagrams. The filled yellow circles and triangles show the current and birth positions, respectively. The red arrow is the motion vector of V454 Aur today. The green and pink dotted lines show the orbit when errors in input parameters are considered, whereas the green and pink filled triangles represent the birth locations of the V454 Aur based on the lower and upper error estimates.

binary system was determined as $R_{\rm Birth} = 8.52 \pm 0.02$ kpc. These findings represent that the V454 Aur was born almost in the solar-abundance region around the Solar circle.

6. CONCLUSIONS

Eclipsing binary systems are the foundation for the studies of stellar astrophysics because they provide accurate stellar parameters that can be used in any area of astrophysics. In this study, we have derived, for the first time, the fundamental parameters of V454 Aur (HD 44192), including temperature, metallicity, and age, by combining photometric radial velocities, precise photometric data, and SED data. We calculated the mass of the components in V454 Aur better than 1.5% as 1.173 $M_\odot$ and 1.045 $M_\odot$ for the primary and secondary component, respectively, and the radii of the components better than 3% as 1.203 $R_\odot$ and 0.993 $R_\odot$ for the primary and the secondary component, respectively. Our distance calculation is in excellent agreement with the *Gaia* DR3 one (Gaia Collaboration et al. 2023), which is in the 2% error range, which indicates that our calculations are accurate. Mass-luminosity parameters that we have derived for the components are slightly smaller than Eker et al. (2018), which is expected considering the position of the V454 Aur on the main sequence. According to our evolution analysis, the components of V454 Aur are still in the main sequence and a little richer than solar metallicity, $z = 0.017$, and the system is far from mass transfer. The initial orbital parameters of the system were derived using the state-of-the-art evolutionary code `MESA` and evolutionary status in several phases were noted in Table 4. According to our calculations, the age of the system is $1.19^{+0.08}_{-0.09}$ Gyr, and it will start mass transfer between components in 5 Gyr when the primary component is in the red giant branch and the secondary component is still on the main-sequence. Calculations of detailed evolutionary steps for eclipsing binaries are important because these calculations generally could shed light on the properties of current semi-detached binaries.

Considering the dynamical orbital parameters and the age of the V454 Aur system, it was determined that it formed in a region around the Solar circle. This result is also consistent with the metal abundance assumed for the V454 Aur. There are still very few systems for which evolutionary phases and birthplaces have been revealed. We believe that determining the initial orbital properties of eclipsing binaries and the location of their birthplaces would help to understand the formation mechanism of eclipsing binaries in detail.

Peer Review: Externally peer-reviewed.

Author Contribution: Conception/Design of study - G.Y., R.C., V.B.; Data Acquisition - G.Y., R.C., V.B.; Data Analysis/Interpretation - G.Y., R.C., V.B.; Drafting Manuscript - G.Y., R.C., V.B.; Critical Revision of Manuscript - G.Y.; Final Approval and Accountability - G.Y.; Technical or Material Support - G.Y.

Conflict of Interest: Authors declared no conflict of interest.

Financial Disclosure: Authors declared no financial support.

Acknowledgements: We are grateful to the anonymous referees for their valuable suggestions. This paper includes data collected with the *TESS* mission, obtained from the MAST data archive at the Space Telescope Science Institute (STScI). Funding for the *TESS* mission is provided by the NASA Explorer Program. STScI is operated by the Association of Universities for Research in Astronomy, Inc., under NASA contract NAS 5–26555. This research has made use of the SIMBAD database, operated at CDS, Strasbourg, France. This work has made use of data from the European Space Agency (ESA) mission *Gaia* (https://www.cosmos.esa.int/gaia), processed by the *Gaia* Data Processing and Analysis Consortium (DPAC, https://www.cosmos.esa.int/web/gaia/dpac/consortium). Funding for the DPAC has been provided by national institutions, in particular, the institutions participating in the *Gaia* Multilateral Agreement. This research has made use of NASA's Astrophysics Data System.

In addition to the Python packages referenced in section 3 and section 4, this research has made use of the following packages: `Astropy` (Astropy Collaboration et al. 2013, 2018, 2022), `corner` (Foreman-Mackey 2016), `Matplotlib` (Hunter 2007), `NumPy` (Harris et al. 2020), and `SciPy` (Virtanen et al. 2020).

LIST OF AUTHOR ORCIDS

G. Yücel	https://orcid.org/0000-0002-9846-3788
R. Canbay	https://orcid.org/0000-0003-2575-9892
V. Bakış	https://orcid.org/0000-0002-3125-9010

REFERENCES

Angulo C., et al., 1999, Nuclear Phys. A, 656, 3

Astropy Collaboration et al., 2013, A&A, 558, A33

Astropy Collaboration et al., 2018, AJ, 156, 123

Astropy Collaboration et al., 2022, ApJ, 935, 167

Bakış V., Eker Z., 2022, Acta Astron., 72, 195

Baranne A., Mayor M., Poncet J. L., 1979, Vistas in Astronomy, 23, 279

Benedict G. F., et al., 2016, AJ, 152, 141

Blouin S., Shaffer N. R., Saumon D., Starrett C. E., 2020, ApJ, 899, 46

Bovy J., 2015, ApJS, 216, 29

Casagrande L., Schönrich R., Asplund M., Cassisi S., Ramírez I., Meléndez J., Bensby T., Feltzing S., 2011, A&A, 530, A138

Cassisi S., Potekhin A. Y., Pietrinferni A., Catelan M., Salaris M., 2007, ApJ, 661, 1094

Chabrier G., 2003, PASP, 115, 763

Chugunov A. I., Dewitt H. E., Yakovlev D. G., 2007, Phys. Rev. D, 76, 025028

Coşkunoğlu B., et al., 2011, MNRAS, 412, 1237

Cyburt R. H., et al., 2010, ApJS, 189, 240

Eggleton P. P., 1983, ApJ, 268, 368

Eker Z., Bakış V., 2023, MNRAS, 523, 2440

Eker Z., et al., 2015, AJ, 149, 131

Eker Z., et al., 2018, MNRAS, 479, 5491

Eker Z., Soydugan F., Bilir S., 2024, arXiv e-prints, p. arXiv:2402.07947

Ferguson J. W., Alexander D. R., Allard F., Barman T., Bodnarik J. G., Hauschildt P. H., Heffner-Wong A., Tamanai A., 2005, ApJ, 623, 585

Foreman-Mackey D., 2016, The Journal of Open Source Software, 1, 24

Foreman-Mackey D., Hogg D. W., Lang D., Goodman J., 2013, PASP, 125, 306

Fuller G. M., Fowler W. A., Newman M. J., 1985, ApJ, 293, 1

Gaia Collaboration et al., 2023, A&A, 674, A1

Griffin R. F., 2001, The Observatory, 121, 315

Harris C. R., et al., 2020, Nature, 585, 357

Holmberg J., Nordström B., Andersen J., 2009, A&A, 501, 941

Hunter J. D., 2007, Computing in Science and Engineering, 9, 90

Hurley J. R., Tout C. A., Pols O. R., 2002, MNRAS, 329, 897

Iglesias C. A., Rogers F. J., 1993, ApJ, 412, 752

Iglesias C. A., Rogers F. J., 1996, ApJ, 464, 943

Irwin A. W., 2004, The FreeEOS Code for Calculating the Equation of State for Stellar Interiors, http://freeeos.sourceforge.net/

Itoh N., Hayashi H., Nishikawa A., Kohyama Y., 1996, ApJS, 102, 411

Jermyn A. S., Schwab J., Bauer E., Timmes F. X., Potekhin A. Y., 2021, ApJ, 913, 72

Jermyn A. S., et al., 2023, ApJS, 265, 15

Johnson D. R. H., Soderblom D. R., 1987, AJ, 93, 864

Kwee K. K., van Woerden H., 1956, Bull. Astron. Inst. Netherlands, 12, 327

Langanke K., Martínez-Pinedo G., 2000, Nuclear Physics A, 673, 481

Leggett S. K., 1992, ApJS, 82, 351

Lightkurve Collaboration et al., 2018, Lightkurve: Kepler and TESS time series analysis in Python, Astrophysics Source Code Library (ascl:1812.013)

Mihalas D., Binney J., 1981, Galactic astronomy. Structure and kinematics

Moe M., Di Stefano R., 2017, ApJS, 230, 15

Nordström B., et al., 2004, A&A, 418, 989

Oda T., Hino M., Muto K., Takahara M., Sato K., 1994, Atomic Data and Nuclear Data Tables, 56, 231

Paegert M., Stassun K. G., Collins K. A., Pepper J., Torres G., Jenkins J., Twicken J. D., Latham D. W., 2022, VizieR Online Data Catalog: TESS Input Catalog version 8.2 (TIC v8.2) (Paegert+, 2021), VizieR On-line Data Catalog: IV/39. Originally published in: 2021arXiv210804778P

Paxton B., Bildsten L., Dotter A., Herwig F., Lesaffre P., Timmes F., 2011, ApJS, 192, 3

Paxton B., et al., 2013, ApJS, 208, 4

Paxton B., et al., 2015, ApJS, 220, 15

Paxton B., et al., 2018, ApJS, 234, 34

Paxton B., et al., 2019, ApJS, 243, 10

Perryman M. A. C., et al., 1997, A&A, 323, L49

Potekhin A. Y., Chabrier G., 2010, Contributions to Plasma Physics, 50, 82

Poutanen J., 2017, ApJ, 835, 119

Prša A., 2020, Contributions of the Astronomical Observatory Skalnate Pleso, 50, 565

Prša A., Zwitter T., 2005, ApJ, 628, 426

Prša A., et al., 2022, ApJS, 258, 16

Rappaport S., Verbunt F., Joss P. C., 1983, ApJ, 275, 713

Ricker G. R., et al., 2015, Journal of Astronomical Telescopes, Instruments, and Systems, 1, 014003

Ritter H., 1988, A&A, 202, 93

Rogers F. J., Nayfonov A., 2002, ApJ, 576, 1064

Rosales J. A., Mennickent R. E., Schleicher D. R. G., Senhadji A. A., 2019, MNRAS, 483, 862

Saumon D., Chabrier G., van Horn H. M., 1995, ApJS, 99, 713

Serenelli A., et al., 2021, A&ARv, 29, 4

Soydugan F., Soydugan E., Aliçavuş F., 2020, Research in Astronomy and Astrophysics, 20, 052

Tasdemir S., Yontan T., 2023, Physics and Astronomy Reports, 1, 1

Timmes F. X., Swesty F. D., 2000, ApJS, 126, 501

Torres G., Andersen J., Giménez A., 2010, A&ARv, 18, 67

Townsend R., 2024, MESA SDK for Linux, doi:10.5281/zenodo.10624843, https://doi.org/10.5281/zenodo.10624843

Tunçel Güçtekin S., Bilir S., Karaali S., Plevne O., Ak S., 2019, Advances in Space Research, 63, 1360

Virtanen P., et al., 2020, Nature Methods, 17, 261

Wilson R. E., 1979, ApJ, 234, 1054

Wilson R. E., 1990, ApJ, 356, 613

Wilson R. E., Devinney E. J., 1971, ApJ, 166, 605

Yontan T., Canbay R., 2023, Physics and Astronomy Reports, 1, 65

Yontan T., et al., 2022, Rev. Mex. Astron. Astrofis., 58, 333

Yücel G., Bakış V., 2022, MNRAS, 516, 2486

van Hamme W., 1993, AJ, 106, 2096

van Hamme W., Wilson R. E., 2003, in Munari U., ed., Astronomical Society of the Pacific Conference Series Vol. 298, GAIA Spectroscopy: Science and Technology. p. 323